Electronic Supplementary Material (ESI) for Physical Chemistry Chemical Physics.
This journal is © the Owner Societies 2021

Electronic Supplementary Information

Gas Phase Ion Chemistry of Titanium-Oxofullerene With Ligated Solvents

*Jayoti Roy[‡], Papri Chakraborty[‡], Ganesan Paramasivam, Ganapati Natarajan[$], and Thalappil Pradeep**

DST Unit of Nanoscience (DST UNS) & Thematic Unit of Excellence (TUE), Department of Chemistry, Indian Institute of Technology Madras, Chennai 600036, India.

International Centre for Clean Water (ICCW), IIT Madras Research Park, Taramani, Chennai 6000113, India.

Table of Contents

List of Figures	Description	Page Number
Fig. S1	UV-vis absorption spectrum of TOF	S3
Fig. S2	Expanded mass spectra	S4
Fig. S3	CID mass spectrum with increasing collision energy	S5
Fig. S4	CID mass spectra with increase of collision energy	S6
Fig. S5	CID mass spectra at larger collision energies	S7
Fig. S6	CID mass spectrum of $[H_{12}Ti_{42}O_{60}(OCH_3)_{42}(HOCH_3)_{10}(H_2O)_2]^{2-}$ at 400 CE	S8
Fig. S7	Expanded views of the calculated and experimental isotopic distributions of Ti-O cage fragments	S9
Fig. S8	CID mass spectra of $[H_7Ti_{42}O_{60}(OCH_3)_{42}(HOCH_3)_{10}(H_2O)_3]^{1-}$ at varying collision energy	S10
Fig. S9	Stacked mass spectra of 1 at 200 CE and 2 at 400 CE	S11
SI1	Additional details of computational study	S11

Fig. S10	Theoretically optimized structures of **1**	S12
SI2	Explanation for the difference in charges between protonated and unprotonated $[Ti_{42}O_{60}(MeO)_{42}(MeOH)_{10}(H_2O)_2]$	S12
S11	Various binding modes and types of electron donation of the methoxide ligand with the Ti1 centre, obtained from DFT models	S12
S12	Theoretically optimized structure of $[H_{12}Ti_{42}O_{60}(CH_3O)_{42}(CH_3OH)_{10}(H_2O)_2\}^{2-}$	S13
S13	Theoretically optimized structures of intermediates (i) $\{H_{12}Ti_{42}O_{60}(CH_3O)_{30}(CH_3OH)_{10}(H_2O)_2\}^{2-}$ (ii)$\{H_{12}Ti_{41}O_{58}(CH_3OH)_{10}(H_2O)_2\}^{2-}$	S14
Table S1	Electron count for various constituents of $H_6[Ti_{42}O_{60}(OCH_3)_{42}(OH)_{12}]$	S15
Table S2	Comparison of Bader charges of the caged methanol molecules in cluster **1**. Labels 1, 2, 3, 4, 5, 6, 7, 8, 9 and 10 refer to each of the 10 methanol molecules	S16
Table S3	Comparison of Bader charges of caged water molecules in the isolated molecule case and in cluster **1**	S19
Table S4	Average Bader charges of ligated molecules in [Ti42(μ3-O)60(OCH3)42(OH)12]6- [computed structure for (TOF)] and in cluster 1.	S19

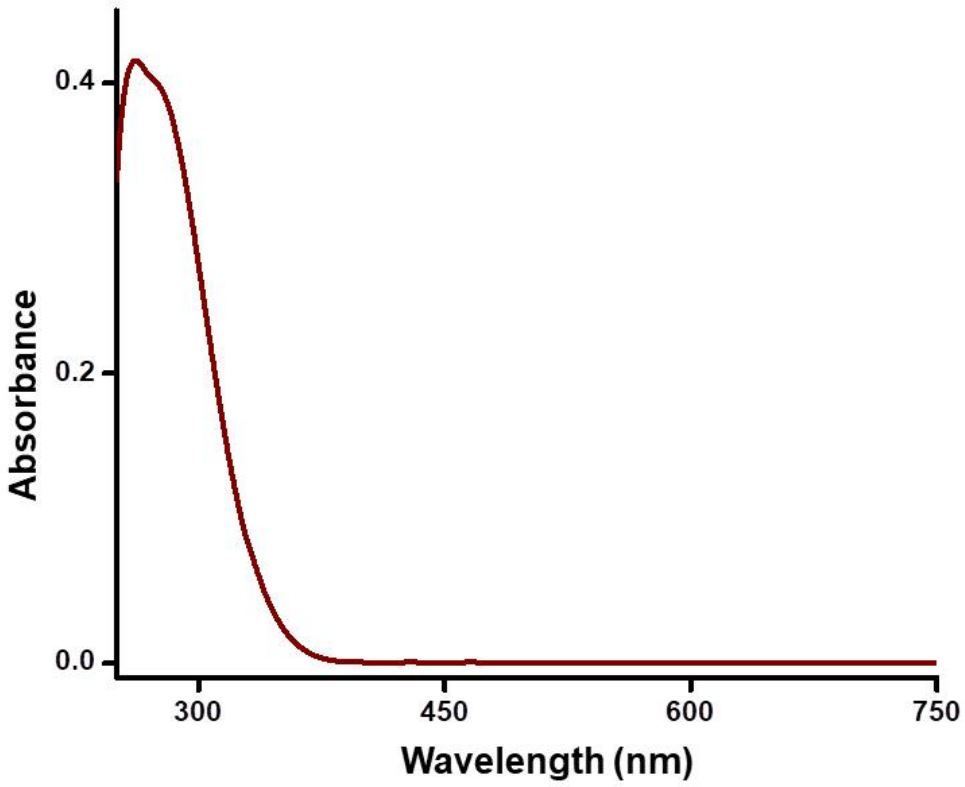

Fig. S1 Solution phase UV-vis absorption spectrum of TOF in toluene.

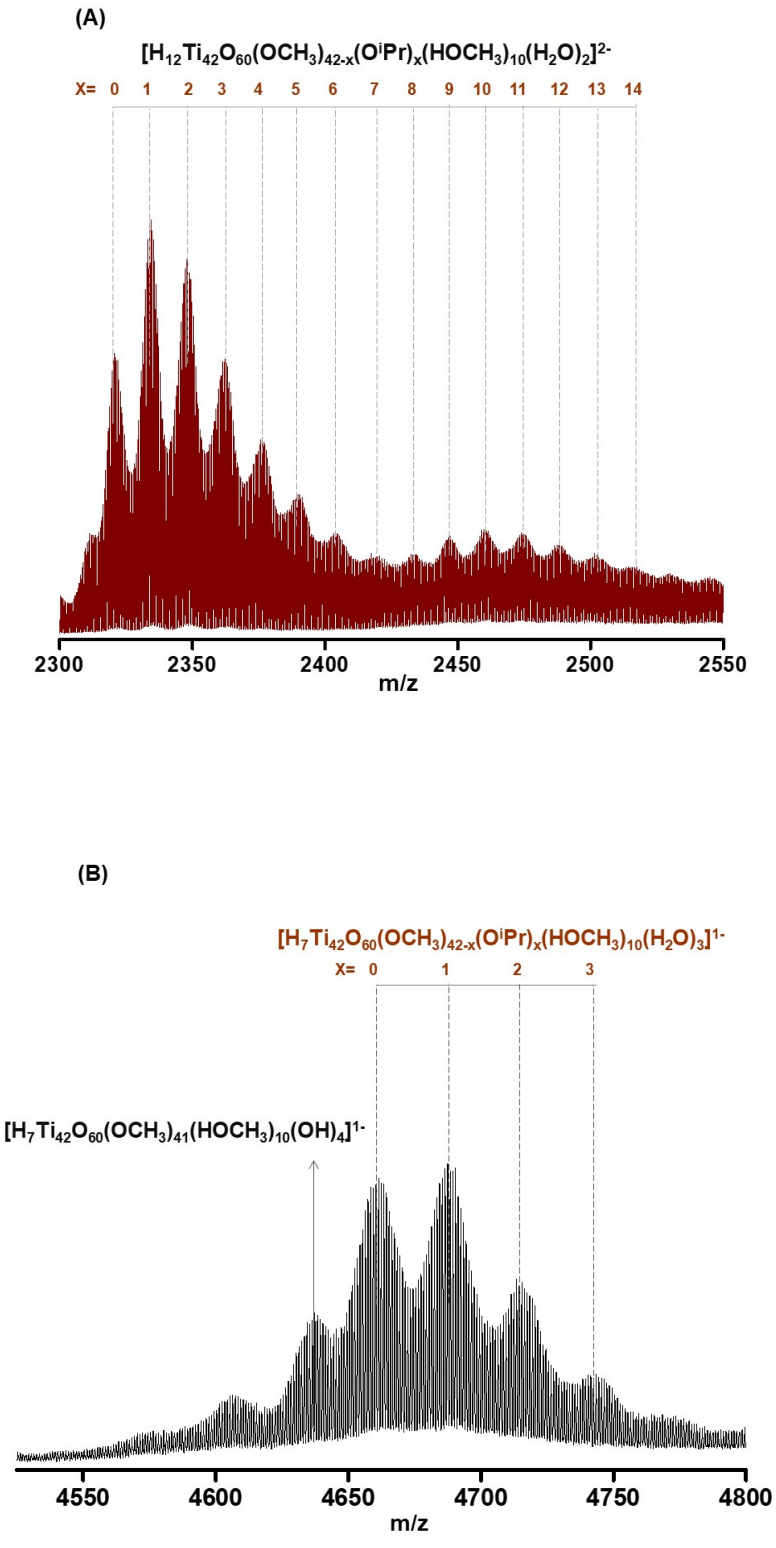

Fig. S2 Expanded view of ESI MS of TOF in the range (A) m/z 2330-2550 and (B) m/z 4525-4800.

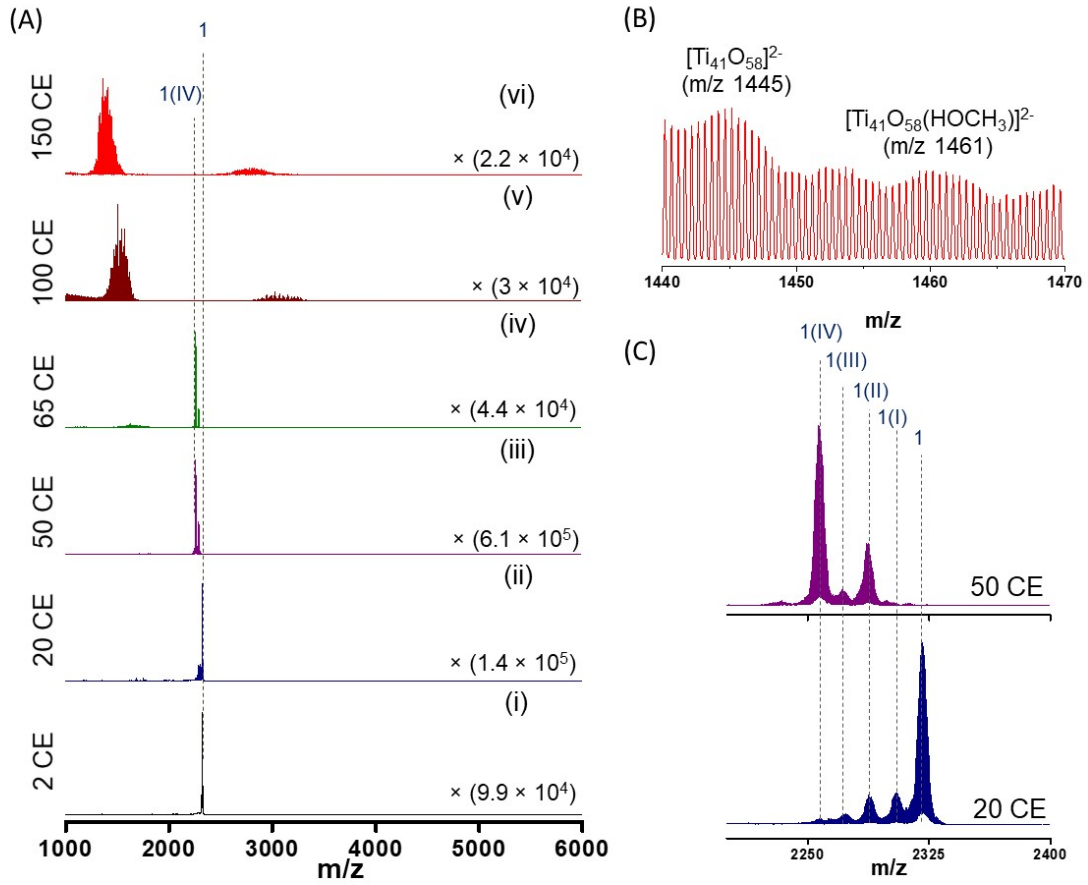

Fig. S3 Detailed CID mass spectrum of $[H_{12}Ti_{42}O_{60}(OCH_3)_{42}(HOCH_3)_{10}(H_2O)_2]^{2-}$ (**1**) with gradual increase of collision energy. (A) MS/MS spectra from 2-150 CE. (B) shows the expanded view of the spectrum at 150 CE in the m/z range of m/z 1440-1470. Mass spectrum of $[Ti_{41}O_{58}]^{2-}$ and $[Ti_{41}O_{58}(HOCH_3)]^{2-}$ are labeled at m/z 1445 and m/z 1461 respectively. (C) shows the expanded spectra in m/z range of 2200-2400 at 20 CE and 50 CE. 1(I), 1(II), 1(III) and 1(IV) correspond to one, two, three, and four methanol loss species from the precursor ion **1**, with molecular formulae $[H_{11}Ti_{42}O_{60}(OCH_3)_{41}(HOCH_3)_{10}(H_2O)_2]^{2-}$, $[H_{10}Ti_{42}O_{60}(OCH_3)_{40}(HOCH_3)_{10}(H_2O)_2]^{2-}$, $[H_9Ti_{42}O_{60}(OCH_3)_{39}(HOCH_3)_{10}(H_2O)_2]^{2-}$, $[H_8Ti_{42}O_{60}(OCH_3)_{38}(HOCH_3)_{10}(H_2O)_2]^{2-}$, respectively.

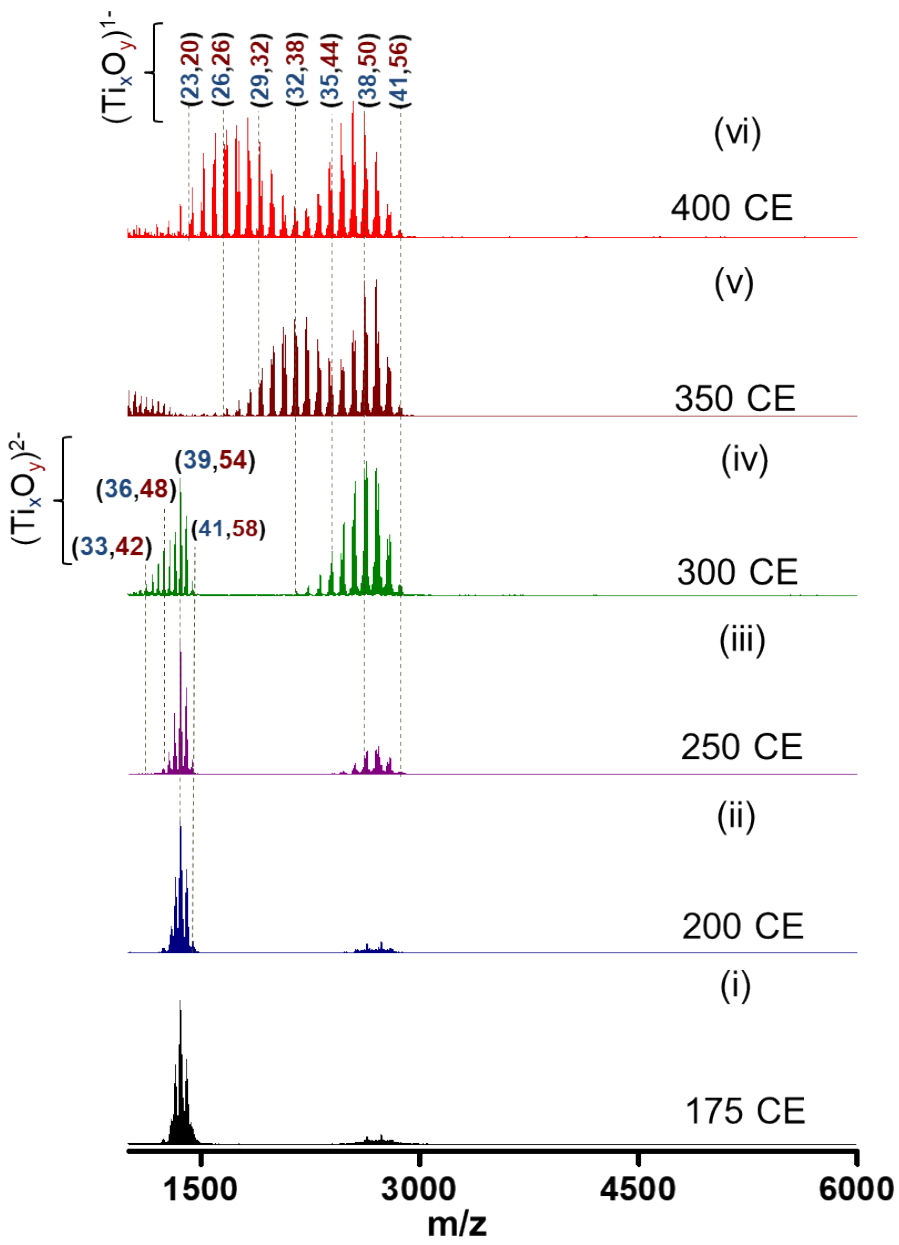

Fig. S4 Detailed CID mass spectrum of $[H_{12}Ti_{42}O_{60}(OCH_3)_{42}(HOCH_3)_{10}(H_2O)_2]^{2-}$ (**1**) with the gradual increase of CE from 175- 400 CE.

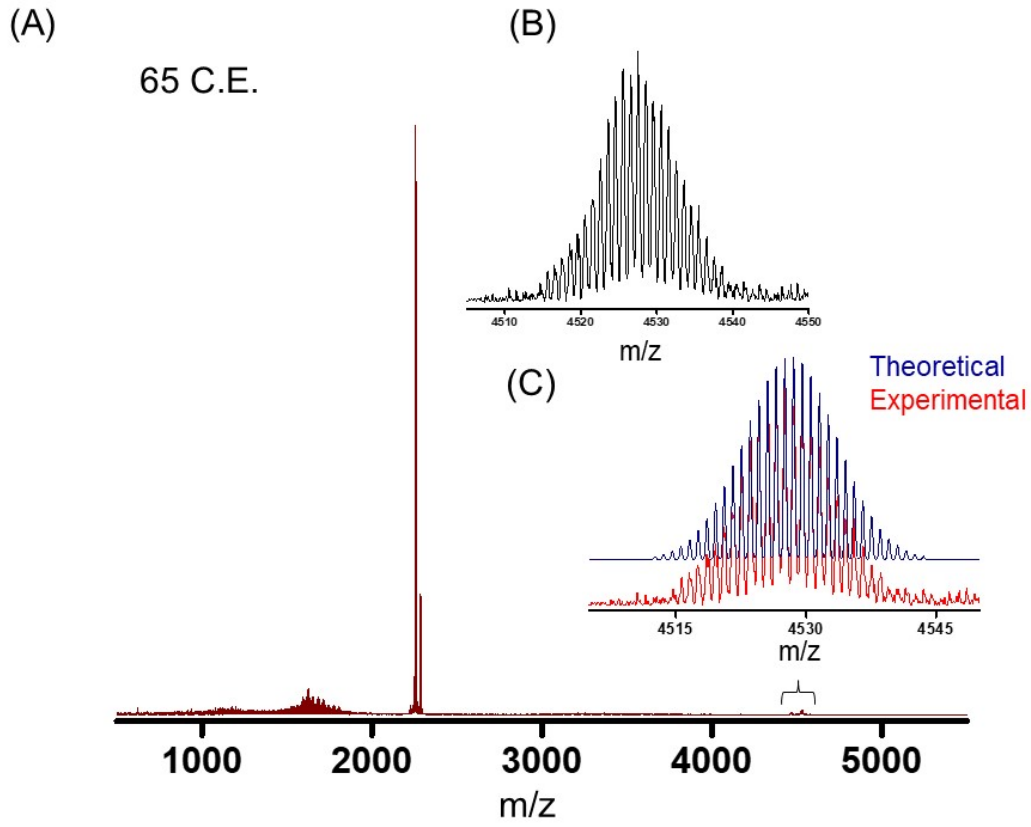

Fig. S5 (A). CID mass spectrum of $[H_{12}Ti_{42}O_{60}(OCH_3)_{42}(HOCH_3)_{10}(H_2O)_2]^{2-}$ at 65 C.E. (B) Expanded view of mass spectrum of $[H_7Ti_{42}O_{60}(OCH_3)_{38}(HOCH_3)_{10}(H_2O)_3]^{1-}$. (C) Theoretical and experimental mass spectrum of $[H_7Ti_{42}O_{60}(OCH_3)_{38}(HOCH_3)_{10}(H_2O)_3]^{1-}$.

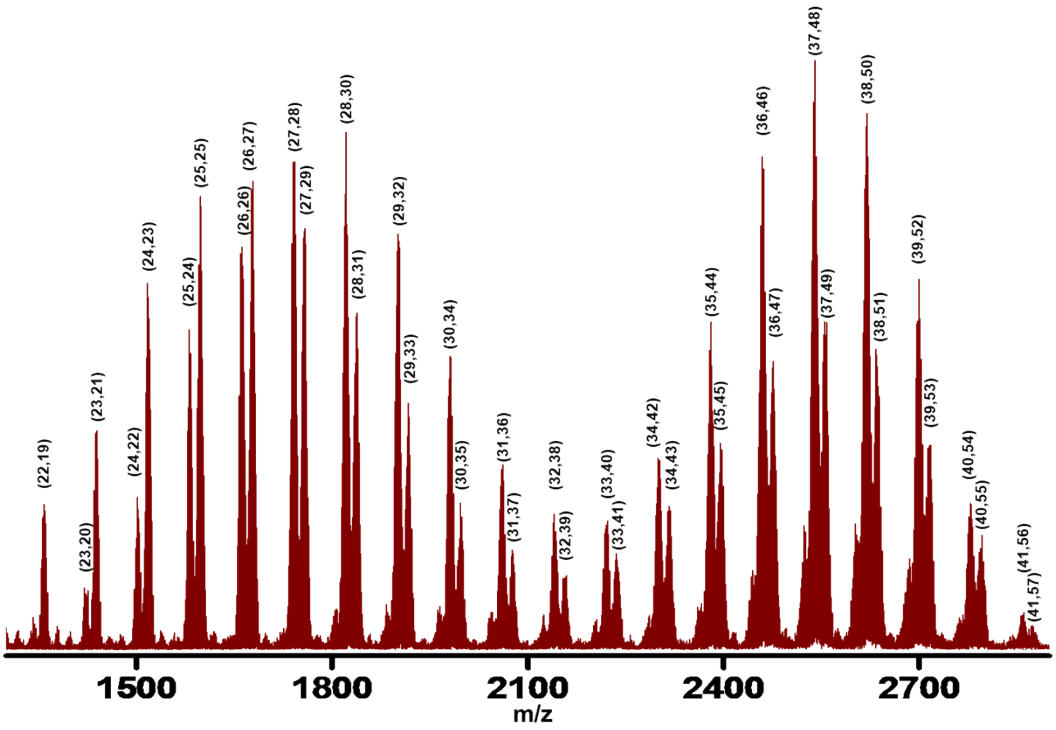

Fig. S6 CID mass spectrum of $[H_{12}Ti_{42}O_{60}(OCH_3)_{42}(HOCH_3)_{10}(H_2O)_2]^{2-}$ at 400 C.E. A cascade of Ti-oxo cage fragments were generated. The peaks are labeled as (x,y) where x and y represent the number of Ti and O atoms present in the cage fragments.

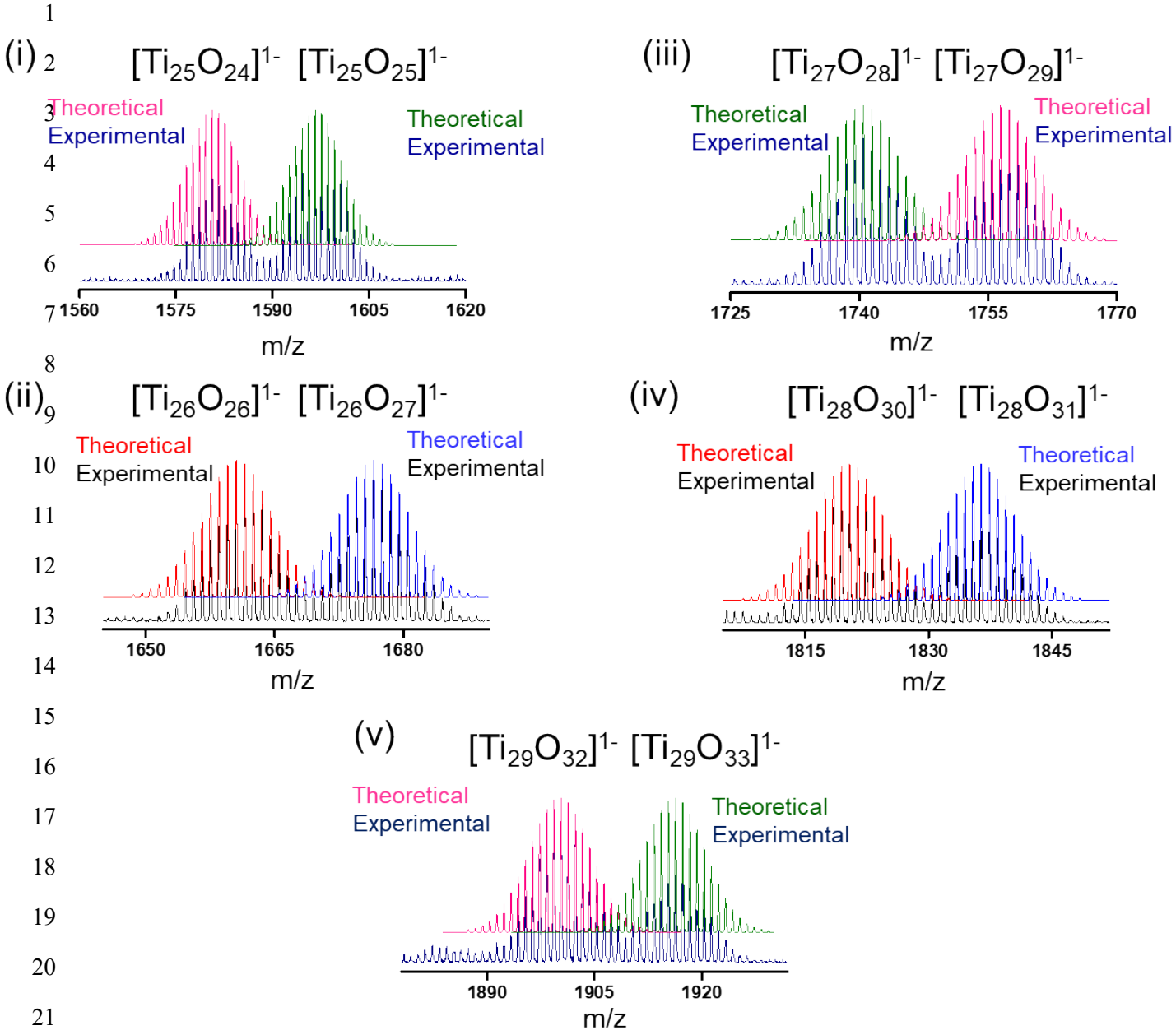

Fig. S7 Expanded views of the calculated and experimental isotopic distributions of (i) $[Ti_{25}O_{24}]^{1-}$, $[Ti_{25}O_{25}]^{1-}$; (ii) $[Ti_{26}O_{26}]^{1-}$, $[Ti_{26}O_{27}]^{1-}$; (iii) $[Ti_{27}O_{28}]^{1-}$, $[Ti_{27}O_{29}]^{1-}$; (iv) $[Ti_{28}O_{30}]^{1-}$, $[Ti_{28}O_{31}]^{1-}$ and (v) $[Ti_{29}O_{32}]^{1-}$, $[Ti_{29}O_{33}]^{1-}$.

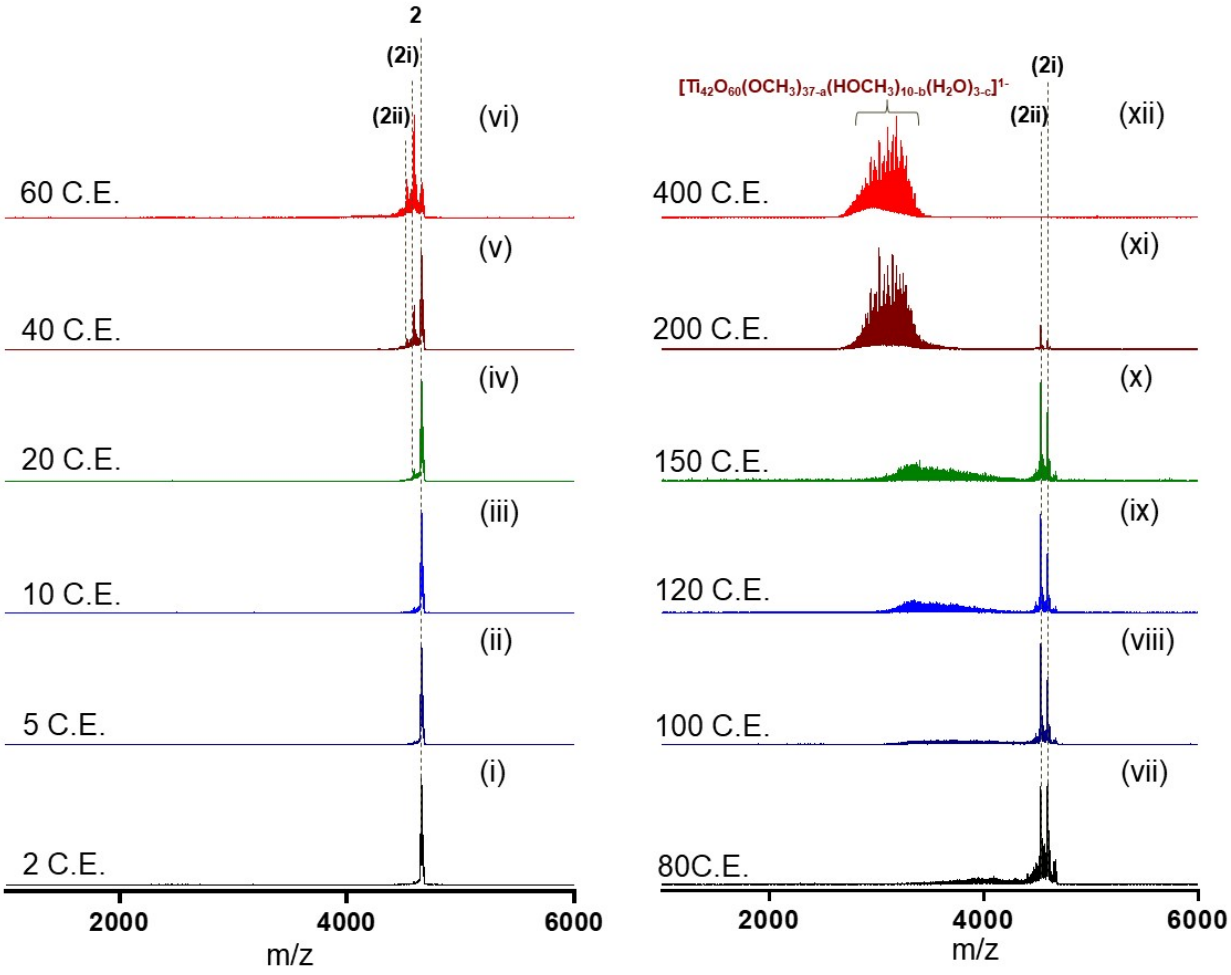

Fig. S8 CID mass spectra of $[H_7Ti_{42}O_{60}(OCH_3)_{42}(HOCH_3)_{10}(H_2O)_3]^{1-}$(**2**) with gradual increase of collision energy from 2 C.E. to 400 C.E. **2i** and **2ii** indicate two and four methanol loss species, respectively from **2**.

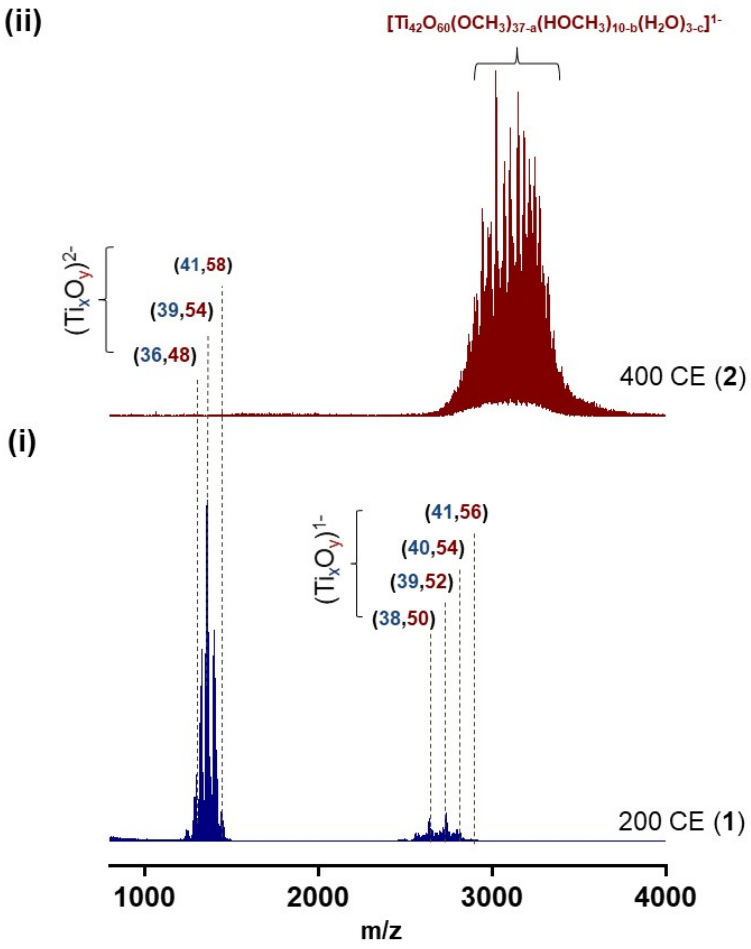

Fig. S9 Stacked mass spectra of parent ions, **1** at 200 CE (i) and **2** at 400 CE (ii).

SI1 Additional details of computational study – DFT calculations were performed with the GPAW method. The atom PAW setups were used as Ti ($3s^2 4s^2 3p^6 3d^2$), O ($2s^2 2p^4$), C ($2s^2 2p^2$), and H($1s^1$) to denote the adequate valance electronic interactions in the calculations. The initial structure of **1** was optimized by taking the crystal structure of TOF, as reported by Gao et al and removing its 6Hs.[1] All geometry optimizations were carried out with a grid spacing of 0.2 A˚ and standard force minimization conditions. PBE exchange functional and double zeta polarization (DZP) basis set were used only because these are accurate enough to give reasonably accuracy for metal cluster systems and are widely used combination in atomic-orbital DFT simulations for nanoclusters.[2–4]

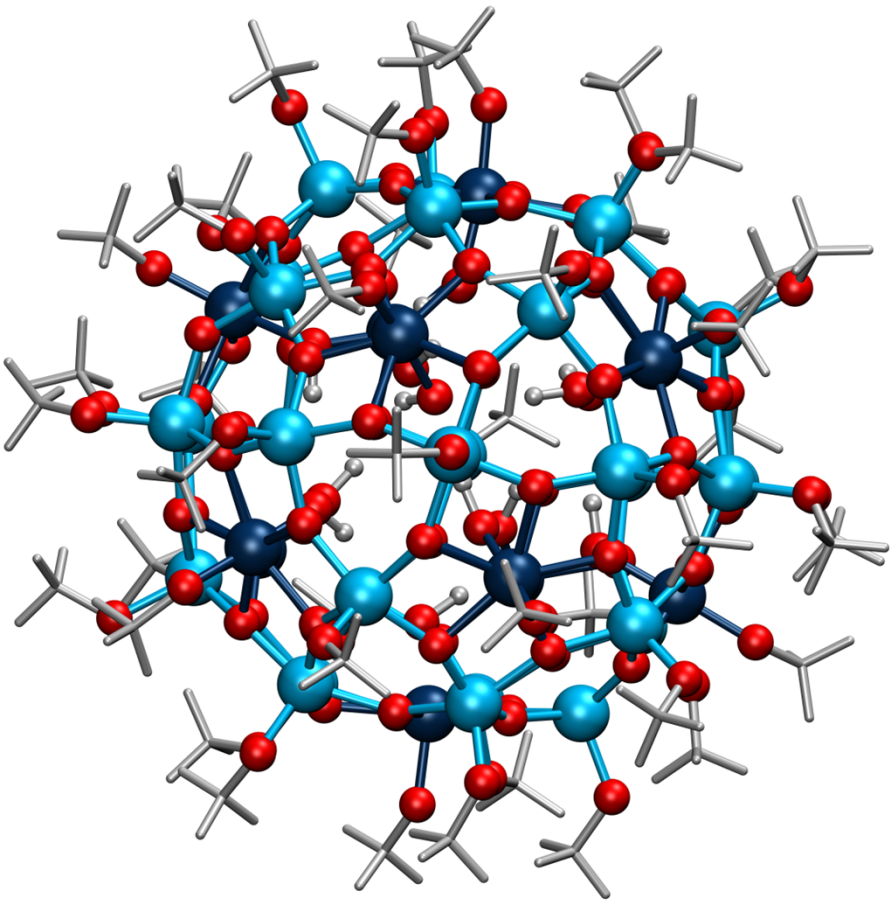

Fig. S10 Theoretically optimized structure of $H_6[Ti_{42}O_{60}(OCH_3)_{42}(OH)_{12}]$, E = -2204.21 eV.

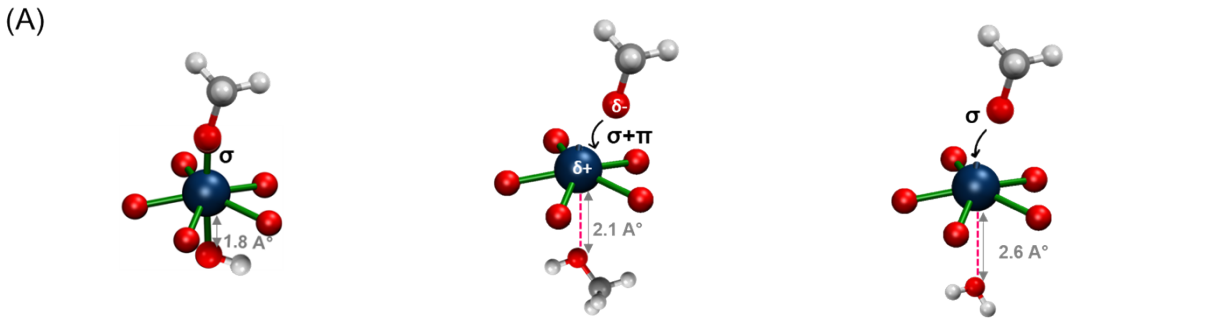

Fig. S11 Various binding modes and types of electron donation of the methoxide ligand with the Ti1 centre, obtained from DFT models. (i) Sigma bonding between methoxide and Ti1 centre of TOF, (ii) sigma and pi electron donation from methoxide ligand to Ti1 atom which is near to methanol molecules in cluster **1** and (iii) only sigma bonding between methoxy and Ti1 centre which is near to the cage-H_2O molecules.

SI2 Explanation of difference in charges between protonated and unprotonated $[Ti_{42}O_{60}(MeO)_{42}(MeOH)_{10}(H_2O)_2]^{-2}$

It is likely that in the gas phase the hydrogen atoms are strongly bonded to the bridging O sites on the surface of the cage, while in the crystal and solution phase the extra hydrogen atoms are more loosely bound to the cluster. This being the case we may treat the twelve H atoms as additional acceptor atoms to the ligands of the cluster. We know from the crystal structure of TOF that there are six preferential sites octahedrally arranged for the six hydrogen atoms though we do not know their exact placement and when we have twelve hydrogen atoms due to symmetry considerations, they will be bonded to the bridging O atoms as six pairs of hydrogen atoms at these six octahedral sites with each H atom donating 1*e*.

We verified that the single-electron donation of H to Ti indeed yields the overall cluster -2 charge according to the standard textbook rules for calculating the charges of organometallic complexes and we only assumed that the two water molecules and ten methanol molecules inside the cage do not donate electrons to Ti. Assuming an oxidation state of 4 for Ti the number of charges on Ti atoms is 42*4*e* = 168*e*. Twelve H atoms are in +1 oxidation state, so electrons accepted by Hs are 12*1*e* = 12*e*. The charges donated by ligands are as following the 10 -OMe ligands (connected to Ti1, close to MeOH) (10x3*e* = 30*e*), 2 -OMe ligands (connected to Ti1, close to H_2O)2*1*e* = *2e*. Remaining 30 -OMe (Ti2 site) ligands and 60 μ_3-bridging atoms donate (30*1*e)* = 30*e,* (60x2*e)* = 120*e* respectively to the Ti atoms. Therefore, total charges donated by ligands is (30+2+30+120)*e* = 182*e* to Ti. Therefore, the charge on the cluster is 168+12-182 = -2.

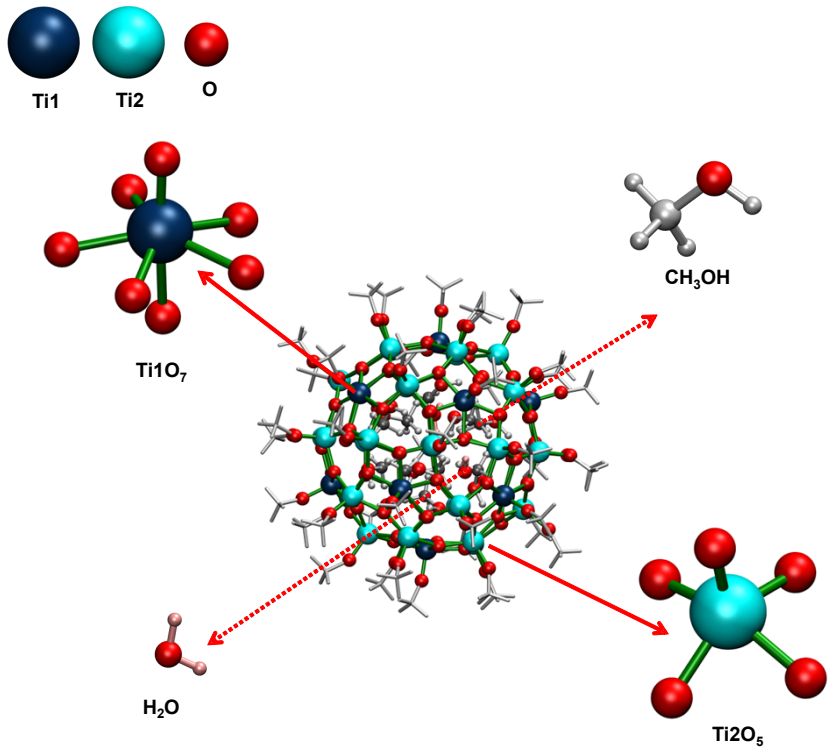

Fig. S12 Theoretically optimized structure of $[H_{12}Ti_{42}O_{60}(CH_3O)_{42}(CH_3OH)_{10}(H_2O)_2\}^{2-}$ (**1**) All constituent molecules such as $Ti1O_7$, $Ti2O_5$, CH_3OH, H_2O are labelled.

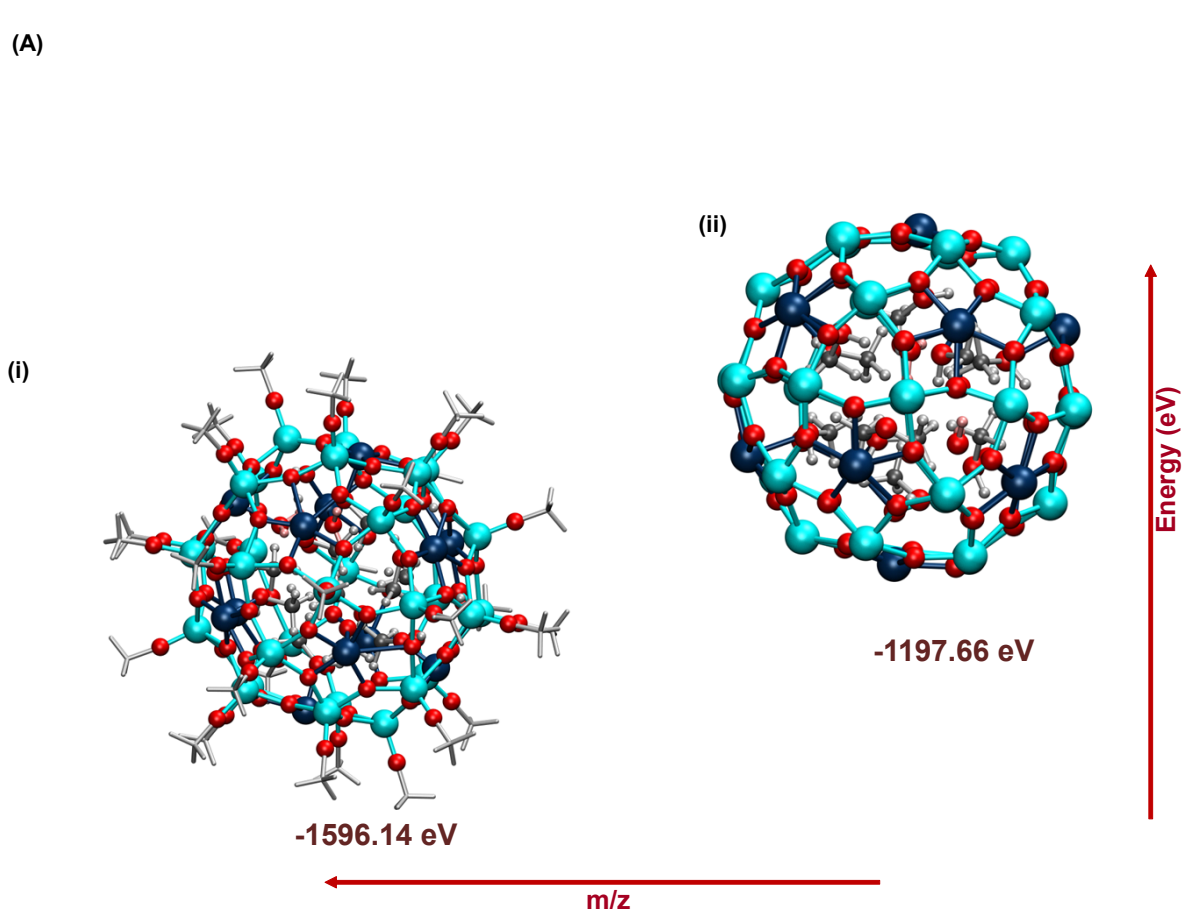

Fig. S13 Theoretically optimized structures of intermediates (i) $[H_{12}Ti_{42}O_{60}(CH_3O)_{30}(CH_3OH)_{10}(H_2O)_2]^{2-}$ (ii) $[H_{12}Ti_{41}O_{58}(CH_3OH)_{10}(H_2O)_2]^{2-}$ formed during gas phase fragmentation.

Table S1 Electron count for various constituents of **1**.

Formula	**No. of electrons donated / lost by each atom**	**No. of ligands/metal atoms**	**Total of charge of electron contribution**	**Total charge (e^-)**
Ti1	4	12	48	180
Ti2	4	30	120	
H	1	12	12	
MeO (Ti1 site close to MeOH)	3	10	-30	-182
MeO (Ti1 site close to H2O)	1	2	-2	
MeO(Ti2 site)	1	30	-30	
μ_3-O	2	60	-120	
$CH_3(OH)$	0	10	0	
H_2O	0	2	0	
Total charge				-2

Table S2: Comparison of Bader charges of the caged methanol molecules in cluster **1**. Labels 1, 2, 3, 4, 5, 6, 7, 8, 9 and 10 refer to each of the 10 methanol molecules.

Atoms	**Isolated methanol (e-)**	**In cluster 1 (e-)**	**Sum of each methanol (e-)**
1) O	-1.073469	-1.125902	
H	0.550502	0.580965	
C	0.405900	0.374355	
H	0.053647	0.122978	
H	0.014493	0.059993	
H	0.048936	-0.018294	-0.005905
2) O		-1.158572	
H		0.612039	
C		0.395603	
H		0.082344	
H		0.000059	
H		0.056760	-0.011767
3) O		-1.143032	
H		0.580766	
C		0.381641	
H		0.005621	
H		0.058059	
H		0.089870	-0.027075
4) O		-1.130505	
H		0.572016	

C		0.341842	
H		0.101267	
H		0.020504	
H		0.086536	-0.00834
5) O		-1.151216	
H		0.590230	
C		0.382089	
H		0.062989	
H		-0.030719	
H		0.090837	-0.05579
6) O		-1.147379	
H		0.589789	
C		0.307513	
H		-0.012398	
H		0.109244	
H		0.095780	-0.057451
7) O		-1.141296	
H		0.581964	
C		0.352674	
H		0.057328	
H		0.024900	
H		0.086162	-0.038268
8) O		-1.151764	
H		0.594026	
C		0.321497	
H		0.105723	
H		0.073583	
H		0.038504	-0.018431
9) O		-1.101824	

Atoms	Isolated water (e-)	In cluster 1 (e-)	Sum of each water (e-)
1) O	-1.094402	-1.174572	
H	0.547159	0.569319	
H	0.547249	0.615906	0.053807
H		0.564074	
C		0.368489	
H		0.019425	
H		0.046601	
10) O		-1.157097	
H		0.602332	
C		0.369650	
H		0.015565	
H		0.040704	
H		0.098016	-0.03083
		Total charge on ten methanol molecules	-0.282348

Table S3: Comparison of Bader charges of caged water molecules in the isolated molecule case and in cluster **1**.

2) O		-1.173333	
H		0.573600	
H		0.576726	-0.023007
		Total charge on both water molecules	-0.012354

Table S4: Average Bader charges of ligated molecules in $[Ti_{42}(\mu^3\text{-}O)_{60}(OCH_3)_{42}(OH)_{12}]^{6-}$ [computed structure for (TOF)] and in cluster **1**.

Atoms	**Average charges in TOF (e-)**	**Average charges in cluster ion 1 (e-)**
OCH_3(Ti1 bonded)	-0.57638	-0.36619
OCH_3(Ti2 bonded)	-0.57511	-0.41631
OH	-0.57386	-
$HOCH_3$	-	-0.0282348
H_2O	-	-0.012354

References

1 M.-Y. Gao, F. Wang, Z.-G. Gu, D.-X. Zhang, L. Zhang and J. Zhang, Fullerene-like Polyoxotitanium Cage with High Solution Stability, *J. Am. Chem. Soc.*, 2016, **138**, 2556–2559.

2 A. H. Larsen, M. Vanin, J. J. Mortensen, K. S. Thygesen and K. W. Jacobsen,

Localized atomic basis set in the projector augmented wave method, *Phys. Rev. B - Condens. Matter Mater. Phys.*, 2009, **80**, 195112.

3 P. Chakraborty, A. Nag, B. Mondal, E. Khatun, G. Paramasivam and T. Pradeep, Fullerene-Mediated Aggregation of $M_{25}(SR)_{18}^-$(M = Ag, Au) Nanoclusters, *J. Phys. Chem. C*, 2020, **124**, 14891–14900.

4 A. Nag, P. Chakraborty, G. Paramasivam, M. Bodiuzzaman, G. Natarajan and T. Pradeep, Isomerism in Supramolecular Adducts of Atomically Precise Nanoparticles, *J. Am. Chem. Soc.*, 2018, **140**, 13590–13593.